Pure appl. geophys. 160 (2003) 1843–1863
0033–4553/03/111843–21
DOI 10.1007/s00024-003-2409-x

Pure and Applied Geophysics

T Waves from the 1998 Papua New Guinea Earthquake and its Aftershocks: Timing the Tsunamigenic Slump

EMILE A. OKAL[1]

Abstract—*T* waves recorded at hydrophone and seismic stations following the Papua New Guinea earthquake of 17 July 1998 and its aftershocks show that a small event at 09:02 GMT featured source properties incompatible with an elastic dislocation of appropriate body-wave magnitude ($m_b = 4.4$). These include an exceptional duration (47 s at the Wake Island hydrophone station WK31), a spectrum rich in high frequencies (7 to 12 Hz), and a generally low spectral amplitude. These characteristics can be explained by the model of an underwater slump, accelerating from a standstill and eventually slowing down. The relocation of the 09:02 event is compatible with its location within an amphitheater inside which shipboard cruises in 1998 and 1999 documented the presence of a 4 – km^3 geologically fresh slump. We propose that the slump took place at 09:02 on 17 July 1998, *i.e.*, 13 minutes after the mainshock, and that it generated the locally catastrophic tsunami, whose properties (amplitude and distribution of runup; timing) could not be explained by a dislocation model.

Key words: *T* waves, landslides, Tsunamis.

1. Introduction

We present in this paper a study of a small aftershock ($m_b = 4.4$; origin time: 09:02 GMT) of the 1998 Papua New Guinea (PNG) earthquake, which we interpret as an underwater slump that generated the locally catastrophic tsunami which followed the earthquake, killing upwards of 2100 people.

We refer to SYNOLAKIS *et al.* (2002) for a discussion of the failure of the main-shock dislocation to properly account for the characteristics of the local tsunami. Briefly summarized, the arguments are of three kinds: First, the runup amplitude observed along the PNG coast ($\zeta = 8$ to 15 m) would require a seismic slip of at least 8 m, in turn incompatible with the seismic moment of the earthquake, which DZIEWONSKI *et al.* (1999) inverted at only $M_0 = 3.7 \times 10^{26}$ dyn-cm. Second, these large runup values are concentrated along a stretch $d = 25$ km of coastline, the aspect ratio ζ/d being incompatible with dislocation models obtained from seismic scaling laws (HOFFMAN *et al.*, 2002). Finally, the arrival time of the tsunami on shore, reconstructed from survivor interviews by DAVIES (1998) to be about 09:10 to 09:12 GMT in the Arop–Malol

[1] Department of Geological Sciences, Northwestern University, Evanston, IL 60208, U.S.A.

area, is too late by at least ten minutes for the mainshock (origin time 08:49) to be its source. By the same token, the main aftershock doublet, at 09:09:32 ($m_b = 5.6$) and 09:10:02 ($m_b = 5.9$) is too late to be an appropriate source of the tsunami.

This failure to explain the local tsunami by a simple elastic dislocation, and in particular the extreme concentration of the high runup amplitudes, suggested, as early as the hours following the disaster, that an underwater landslide or slump may have generated the tsunami. This scenario was supported by shipboard explorations of the area offshore of the Sandaun coast in late 1998 and 1999, which identified and mapped a fresh slump of $\sim$4 km^3 centered in an amphitheater located at 2.83°S and 142.25°E, although obviously no precise time stamp could be put on its occurrence (TAPPIN *et al.*, 1999; SWEET and SILVER, 2003).

In this framework, we investigate in the present paper the seismic events which took place between the mainshock at 08:49 GMT and the main aftershock doublet at 09:09–09:10, and present evidence that an event detected at 09:02 GMT involved a major slump, which we propose as the source of the tsunami. Our evidence is largely based on the T waves recorded at various sites from the 09:02 event.

2. Relocation

The National Earthquake Information Center (NEIC) lists two earthquakes between the main shock and the main aftershock doublet: one at 09:02:06 ($m_b = 4.4$) and one at 09:06:01 (no magnitude reported). We use the technique of WYSESSION *et al.*(1991) to relocate these events, including an assessment of their 95%–confidence ellipses through a Monte Carlo method injecting Gaussian noise (with standard deviation σ_G) into the data set. Note that, while the two events considered are legitimate contenders for the generation of the tsunami in terms of their timing, their size clearly rules out explaining the amplitude of the observed runup as due to any model of those earthquakes as standard dislocations in an elastic medium.

Results, shown on Figure 1, show that the error ellipse of the 09:02 event (computed for $\sigma_G = 1$ s) does include the amphitheater where the slump was mapped during the shipboard surveys (TAPPIN *et al.*, 1999). It is then legitimate to assume that the 09:02 event took place at the location of the observed slump, inside the amphitheater. On the other hand, the 09:06 event could not be meaningfully relocated (Fig. 1), its error ellipse extending more than 150 km in the EW direction.

We also relocated all 57 further aftershocks of the PNG earthquake initially listed in the weekly Preliminary Determination of Epicenter Bulletins for the remainder of the year 1998 (a 166–day interval), in order to assess their error ellipses. Results, listed in Table 1 and shown on Figure 2, indicate a large scatter of the solutions, including in the direction perpendicular to the shoreline, which would be generally compatible with interpreting the shallow-dipping fault plane of the CMT mechanism (DZIEWONSKI

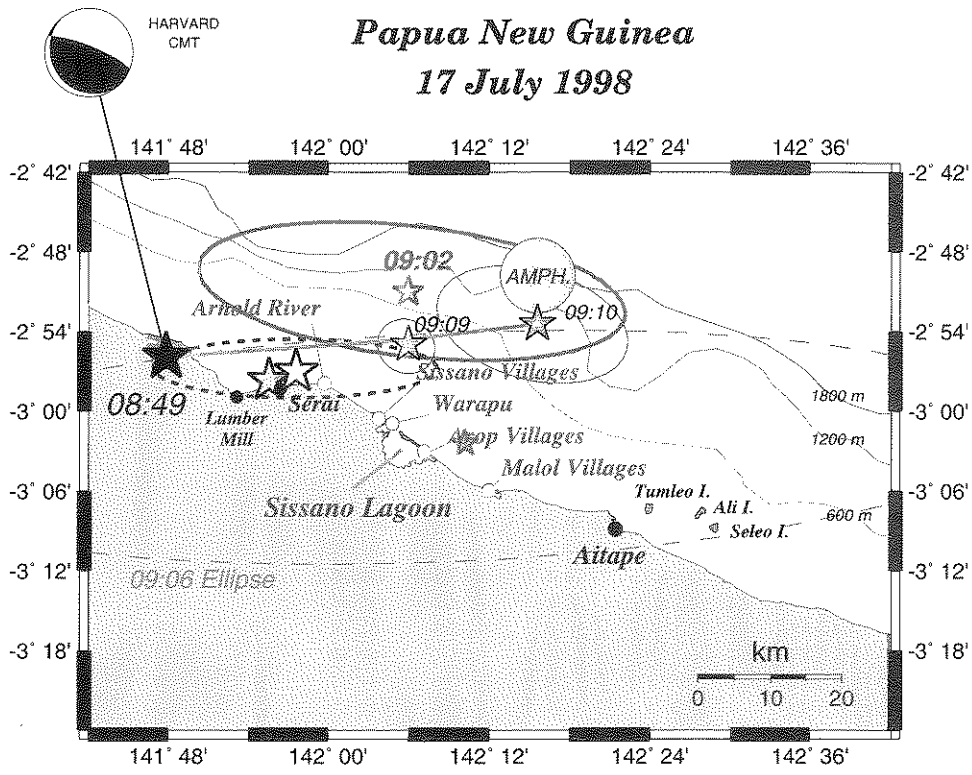

Figure 1

Map of the Sandaun coast of Northwestern Papua New Guinea. The open circles on the coastline identify villages devastated by the tsunami; the solid circles are other, mostly spared, communities. The large stars are epicenters of the mainshock (black: initial NEIC; grey: final NEIC; white: as relocated in this study, with error ellipse (dotted line)). The smaller, grey stars are epicenters of the relocated doublet at 09:09 and 09:10 GMT (with Monte Carlo ellipses). The line joining them is the extent of the seismic rupture, as inferred from the seismological modeling of KIKUCHI *et al.* (1998). The open star is the relocated epicenter of the 09:02 seismic event (with solid-line Monte Carlo ellipse). The superimposed disk labeled "*AMPH.*" schematizes the location of the amphitheater where the slump was identified by the surveys. The smaller gray star if the tentative relocation of the 09:06 event, with its large error ellipse (dashed line).

et al., 1999) as the plane of rupture. These results are essentially identical to those of MCCUE (1998) who combined preliminary NEIC epicenters with data from portable stations operated after 03 August 1998 by the Australian Geological Survey Organization, and of the more recent ones by HURUKAWA *et al.* (2003) who included data from a deployment of three portable stations in August and September 1998.

In addition to the 09:02 and 09:06 events, the records of the broadband Poseidon station at Jayapura, Indonesia (JAY; 2.52°S, 140.70°E; 155 km WNW of Sissano along the coast) feature a strongly impulsive event at 08:58. This event is not documented by the NEIC. Figure 3 shows that its duration at JAY (35 s) is significantly shorter than that of typical aftershocks of small magnitude, such as the

Table 1

Relocation of the PNG earthquake and its principal aftershocks

Date	Origin Time	Magnitude	Epicenter		Number of stations	σ	Length of major axis
D M (J) Y	GMT	m_b	°N	°E		(s)	(km)
17 JUL (198) 1998	08:49:12.7	6.8†	−2.95	141.96	54	1.30	38
17 JUL (198) 1998	09:02:05.7	4.4	−2.85	142.10	13	1.13	63
17 JUL (198) 1998	09:06:00.9		−3.04	142.17	4	0.14	150
17 JUL (198) 1998	09:09:31.2	5.6	−2.91	142.10	99	1.25	8
17 JUL (198) 1998	09:10:01.8	5.9	−2.89	142.26	38	1.13	27
17 JUL (198) 1998	09:19:12.7	4.5	−2.59	142.27	14	1.31	24
17 JUL (198) 1998	09:29:13.5	4.1	−2.82	141.82	17	1.35	23
17 JUL (198) 1998	09:40:07.6	4.5	−2.94	142.12	28	1.21	21
17 JUL (198) 1998	10:21:35.6	3.6	−3.06	142.44	5	0.37	177
17 JUL (198) 1998	11:53:36.9	4.1	−2.70	142.16	21	1.11	24
17 JUL (198) 1998	12:15:09.0	3.2	−2.99	142.47	6	0.34	156
17 JUL (198) 1998	12:59:59.5	3.9	−3.04	142.55	12	1.61	55
17 JUL (198) 1998	13:02:24.2	4.2	−2.69	142.27	15	1.00	39
17 JUL (198) 1998	13:12:56.5	4.2	−2.90	141.97	11	1.12	48
17 JUL (198) 1998	13:16:44.1	4.4	−2.75	142.16	25	0.72	22
17 JUL (198) 1998	13:32:55.4	4.4	−3.02	142.43	7	0.51	146
17 JUL (198) 1998	13:52:55.9	4.5	−3.00	142.26	32	2.11	16
17 JUL (198) 1998	15:46:35.9	3.8	−2.67	142.40	9	0.28	62
17 JUL (198) 1998	17:17:57.1	3.6	−2.76	141.87	11	1.64	27
17 JUL (198) 1998	17:19:23.8	4.3	−3.16	142.83	12	1.44	46
17 JUL (198) 1998	17:39:45.6	4.4	−2.99	142.13	21	1.29	18
17 JUL (198) 1998	18:17:14.4	4.7	−2.89	142.10	38	0.95	15
17 JUL (198) 1998	18:36:36.1	4.5	−2.89	142.18	28	1.14	16
17 JUL (198) 1998	18:50:42.0	4.7	−2.92	142.28	32	1.10	19
17 JUL (198) 1998	19:03:52.2		−2.76	142.37	5	0.34	74
17 JUL (198) 1998	20:19:56.4	4.1	−2.73	142.05	9	0.57	47
18 JUL (199) 1998	01:32:37.7	4.5	−2.91	142.16	34	1.07	25
18 JUL (199) 1998	01:41:11.5	4.9	−2.76	142.06	41	1.10	16
18 JUL (199) 1998	08:19:00.8	4.4	−2.92	141.87	20	1.66	34
18 JUL (199) 1998	09:23:34.7	4.4	−2.77	141.96	31	1.13	21
18 JUL (199) 1998	19:52:02.9	4.9	−2.61	142.14	6	0.79	86
19 JUL (200) 1998	08:47:05.7	4.8	−2.52	142.04	62	1.29	9
19 JUL (200) 1998	16:57:40.2	4.6	−2.92	142.16	35	1.31	13
19 JUL (200) 1998	19:44:53.8	4.4	−2.97	141.98	7	0.69	26
21 JUL (202) 1998	16:29:51.1	4.4	−2.89	142.42	28	0.94	17
22 JUL (203) 1998	06:30:50.2	4.4	−2.92	142.19	21	1.33	21
22 JUL (203) 1998	09:21:18.5	4.5	−3.05	141.79	31	0.90	16
22 JUL (203) 1998	10:09:51.5	4.8	−3.10	141.76	44	0.90	12
22 JUL (203) 1998	22:42:48.4	4.3	−3.10	142.21	23	1.33	17
24 JUL (205) 1998	17:11:54.3	5.0	−2.84	142.13	70	1.15	10
24 JUL (205) 1998	23:58:27.8	4.9	−2.82	142.38	5	0.56	40
25 JUL (206) 1998	17:36:49.9	4.6	−2.76	142.06	19	1.04	21
26 JUL (207) 1998	02:09:57.7	4.0	−2.92	141.66	10	1.15	35
26 JUL (207) 1998	02:30:25.5	3.4	−2.76	142.00	7	1.07	40
26 JUL (207) 1998	08:49:22.5		−2.95	141.92	5	0.32	36
27 JUL (208) 1998	01:56:03.3	3.7	−2.80	142.32	8	1.00	28

Table 1

Contd

Date	Origin Time	Magnitude	Epicenter		Number of stations	σ	Length of major axis
D M (J) Y	GMT	m_b	°N	°E		(s)	(km)
27 JUL (208) 1998	05:25:53.8	4.5	−2.67	142.75	6	0.60	38
02 AUG (214) 1998	07:35:12.7	4.5	−2.79	142.79	23	1.32	20
09 AUG (221) 1998	18:40:10.3	4.7	−2.84	141.95	26	1.08	23
22 AUG (234) 1998	11:09:45.1	5.4	−3.06	142.03	100	1.20	9
25 AUG (237) 1998	12:37:12.4	4.4	−2.99	142.26	11	0.78	22
26 AUG (238) 1998	02:04:44.9	4.8	−2.93	142.19	43	1.15	13
26 SEP (269) 1998	22:12:31.1	4.4	−2.91	141.51	16	0.94	29
28 SEP (271) 1998	23:41:37.0	4.1	−2.97	141.87	13	0.89	24
11 OCT (284) 1998	10:00:10.9	4.6	−2.93	142.16	22	1.12	17
11 OCT (284) 1998	14:35:01.3	4.7	−2.94	142.01	46	1.20	12
21 OCT (294) 1998	05:30:52.4	3.7	−3.26	142.77	21	0.85	18
25 NOV (329) 1998	05:19:15.2	4.3	−2.90	141.64	19	0.86	25
29 DEC (363) 1998	01:22:11.6	4.7	−3.04	141.91	8	0.93	28

† Magnitude M_m (OKAL and TALANDIER, 1989).

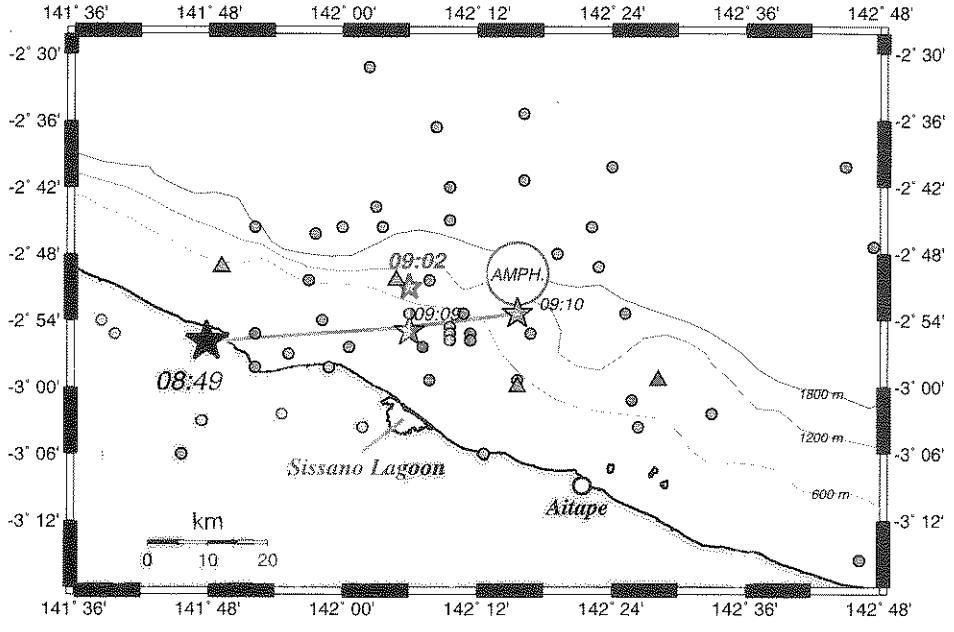

Figure 2

Map of aftershocks of the PNG sequence. The solid dots are the relocated epicenters listed in Table 1. Stars as in Figure 1. The four triangles identify those events which featured *T* wavetrains of longer duration at hydrophone station WK31.

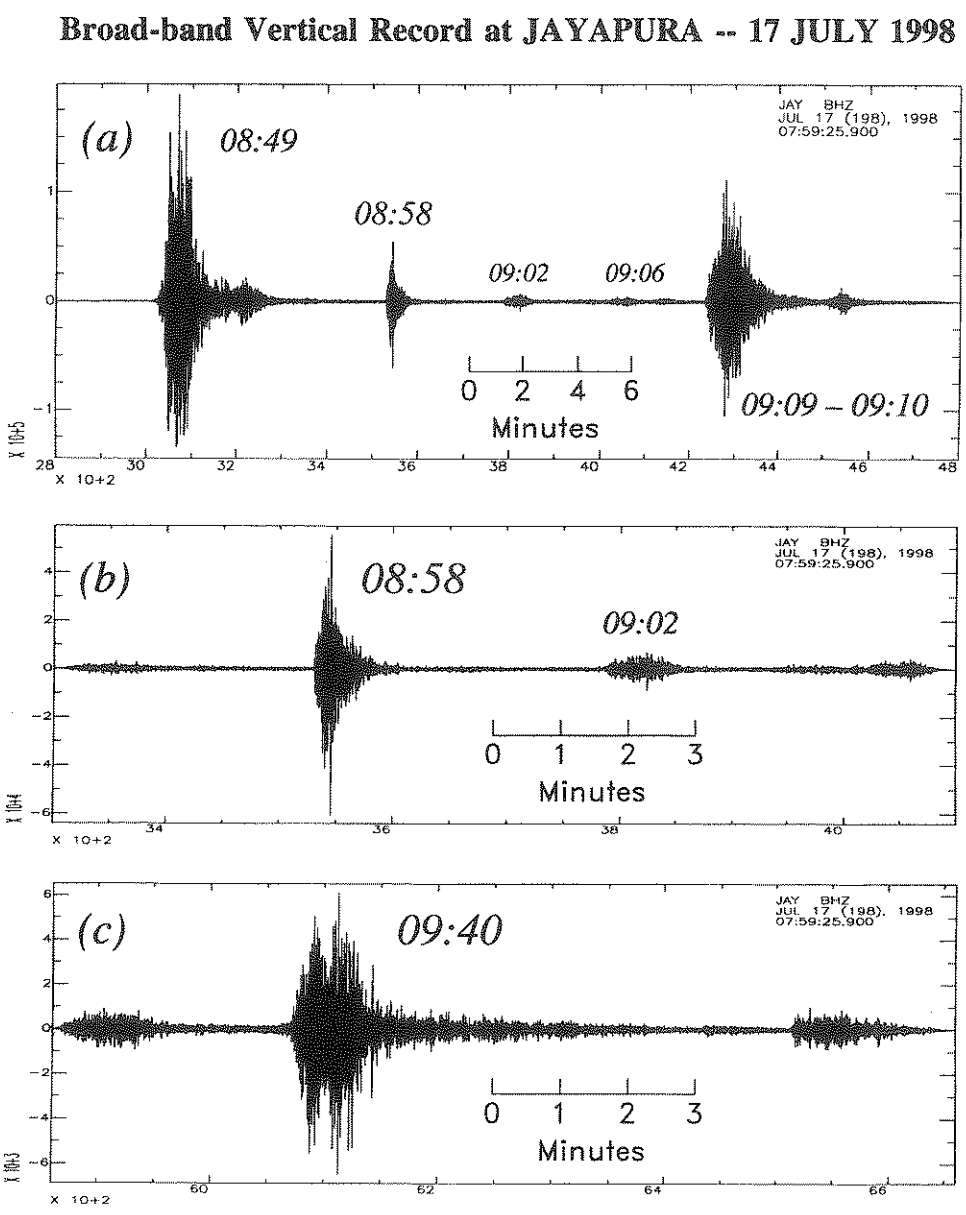

Figure 3

Broadband vertical record at the POSEIDON station JAY (Jayapura, Indonesia). All three frames have been highpass filtered at 1 Hz. Arrivals are identified by the origin time of the corresponding events. (a): 2000-second window showing P_n arrivals from the mainshock (08:49) and main aftershock doublet (09:09–09:10). Note that, in addition to the 09:02 and 09:06 events, this record shows a prominent arrival at 08:58. (b): 800-second window showing a close-up of the 08:58 arrival. Note impulsive nature and short duration of the wavetrain, as compared to the case of the 09:40 aftershock shown on Frame (c).

09:40 aftershock (70 s; $m_b = 4.5$), which we relocated at 2.94°S, 142.12°E, 165 km from JAY. In addition, the 08:58 event has a sharp impulsive arrival at JAY, characteristic of crustal propagation, as compared to the classically emergent nature of P_n wavetrains observed for the regular aftershocks. Finally, the spectrum of the 08:58 wavetrain is richer in intermediate-to-high frequencies (f = 2–4 Hz) than that of the 09:40 shock, advocating lesser attenuation, and hence a shorter path to JAY. While it was not possible to formerly relocate the 08:58 event, these characteristics of the JAY record suggest an epicentral distance no greater than 100 km and thus rule it out as a direct aftershock of the PNG earthquake located in the rupture area of the mainshock, and *a fortiori* as a source of the tsunami.

3. T-wave Records of the 09:02 Event

The small shocks at 09:02 and 09:06 GMT were recorded by very few stations (13 and 4, respectively), and their conventional seismic records are of relatively poor quality, especially in the near-field. For this reason, and in order to investigate their sources, we now turn to the *T* waves generated by the PNG aftershocks. We recall that *T* waves are acoustic (sound) waves generated in the water column of the world's oceans by a variety of sources including oceanic earthquakes, and efficiently propagated to extreme distances on account of the channeling properties of the SOFAR waveguide (EWING *et al.*, 1946). They can be recorded either at sea on hydrophones or by seismometers deployed close to shorelines, through their conversion to seismic waves when they hit the shore (*e.g.*, OKAL, 2001a).

• *The Wk31 record*

Figure 4 is a plot of the time series recorded at Hydrophone WK31, located 175 km SSE of Wake Island, at a distance of 3600 km from the amphitheater. The record has been filtered in the frequency band $1 < f < 30$ Hz. Apart from the prominent wavetrains from the mainshock and main aftershock doublet, *T* waves from the 09:02 and 09:06 events (arriving at 09:42 and 09:46, respectively) are readily identified. Even on this unprocessed record, there is a hint of a longer duration of the 09:02 *T* wavetrain. This is confirmed by the spectrograms shown on Figure 5, which reveal some exceptional characteristics of this wavetrain.

* *Duration*

First, the duration of the *T* wave at WK31 is approximately 47 seconds. As documented on Figure 5b, this is comparable to the duration of *T* waves from the mainshock ($m_b = 5.9; M_0 = 3.7 \times 10^{26}$ dyn-cm) and three times that of aftershocks of comparable magnitude (*e.g.*, 09:40 GMT; $m_b = 4.5$; Figure 5c). Note that the duration which can be measured on self-scaling plots such as the spectrograms on Figure 5, represents the duration of sustained energy at a given level of attenuation

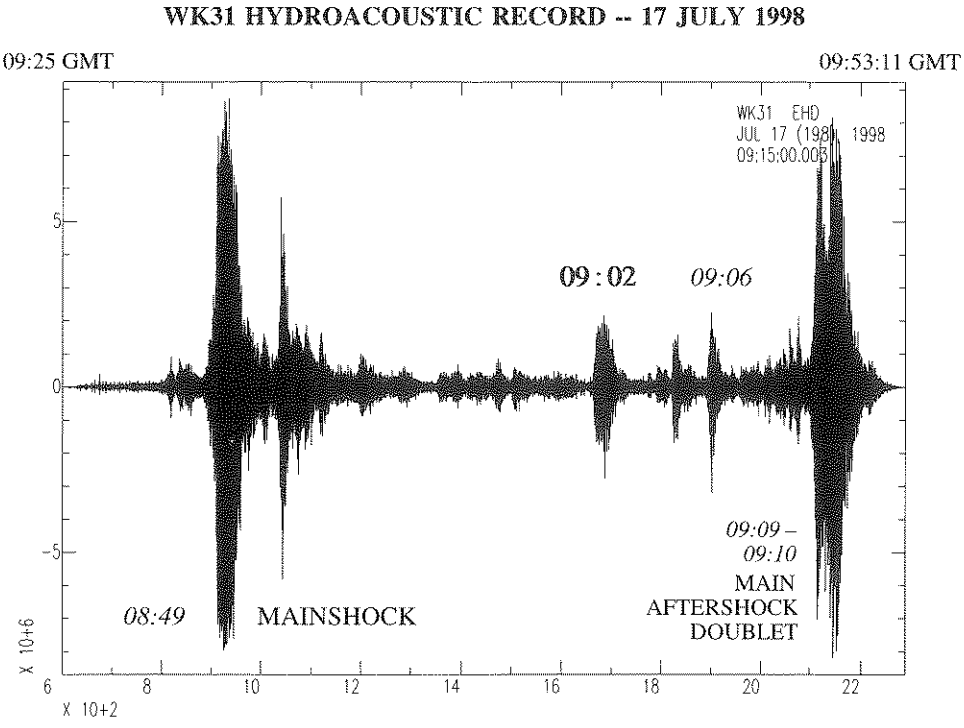

Figure 4

T-wave record of the PNG sequence at hydroacoustic station WK31. This record has been bandpass filtered between 1 and 30 Hz, in order to eliminate electrical noise contaminating the original time series at 60 Hz. The various events are identified on the record by their origin time. Note that the longer duration of the 09:02 event can be detected on this record (as compared for example with the 09:06 shock). Note also the absence of any *T*-wave signal for the 08:58 event recorded at JAY (see Fig. 3), suggesting the latter has a different epicenter, outside the rupture area of the mainshock.

from its peak value (in practice $\approx$ 40 dB). In terms of characterizing the duration of the source process, this concept is more robust than the use of an absolute threshold; for example, a similar approach was used for discrimination purposes on *T*–phase signals by TALANDIER and OKAL (2001).

Figure 5

Time series and spectrograms of *T* waves received from the PNG sequence at the hydrophone station WK31 of the PIDC. All time series are 120-s long. The 09:02 event ($m_b = 4.4$) interpreted as the tsunami-generating slump is shown at the top (a), and compared to the mainshock (b) and an aftershock at 09:40, with comparable magnitude and location (*c*; $m_b = 4.5$). The spectrograms contour the energy present in the signal as a function of time (abscissa) and frequency (ordinate). Note the exceptional duration (47 s) of the 09:02 signal. The duration of the mainshock *T* wave is not affected by the obvious amplitude saturation of the signal.

The duration of a *T* wave recorded by a hydrophone can be expected to be controlled by (i) the duration of the seismic source itself, which is a combination of rise time and rupture time; (ii) different modes of seismic propagation before

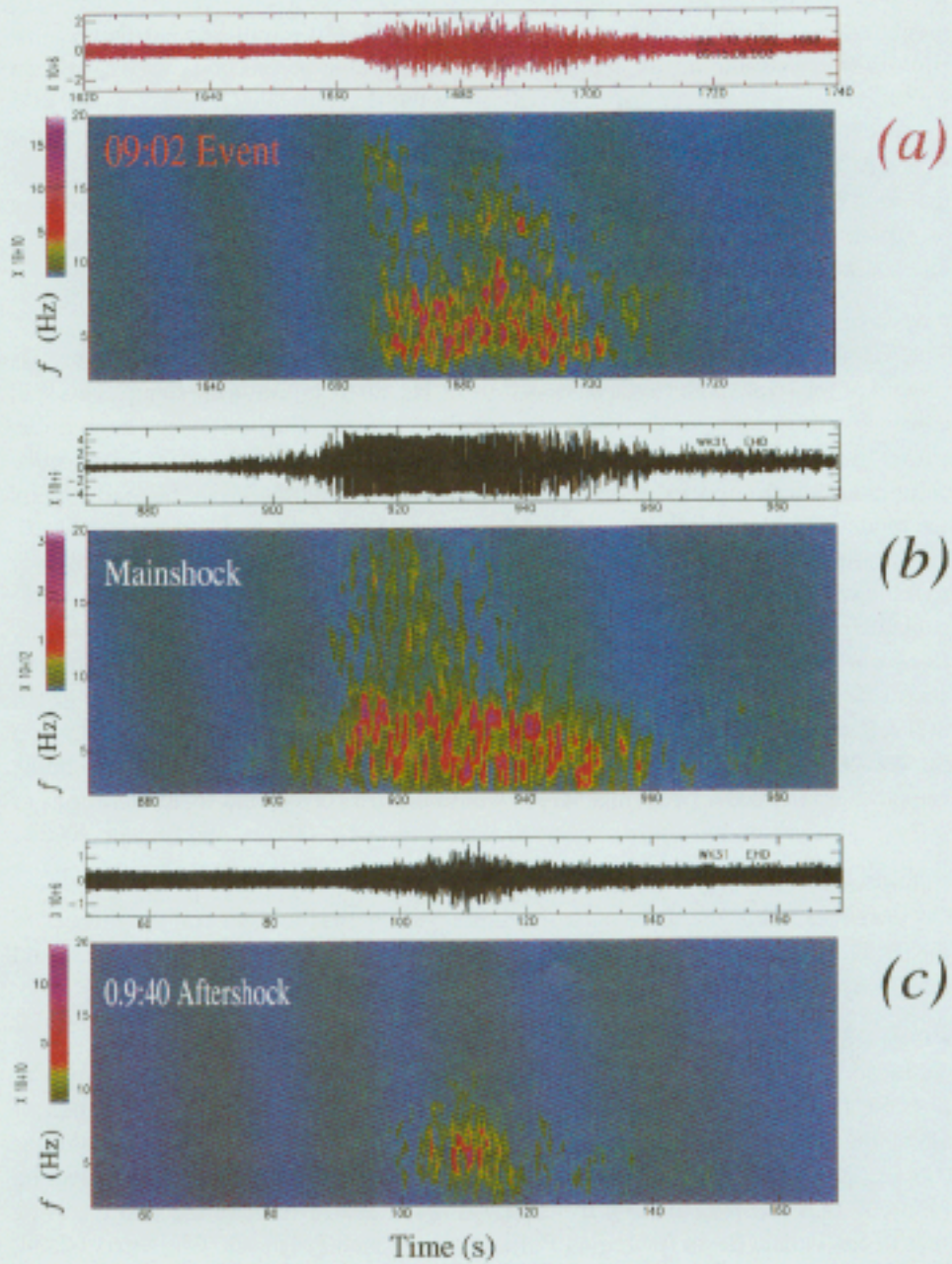

conversion to an acoustic wave in the water, such as a difference in travel time for *P* or *S* segments in the solid earth, as well as multipathing along different seismic paths; and (iii) the intrinsic dispersion of the acoustic wave in the water. Parameters (ii) and (iii) would not be expected to vary significantly between aftershocks, and certainly not to extend the duration of the wavetrain to 45 seconds. Matching a 1-s body-wave magnitude of 4.4 with a duration of 45 s or more would require an extremely slow rupture which would in turn give rise to substantial long-period body waves, or even surface waves, which were not observed for the 09:02 event. Such a source would also be an extremely poor generator of the high frequencies necessary to penetrate the SOFAR channel; indeed the so-called "tsunami earthquakes" are notoriously deficient *T*-wave generators (OKAL *et al.*, 2003). In summary, there is simply no way to explain the duration of the 09:02 *T*-wavetrain at WK31 with the simple model of an elastic dislocation compatible with earthquake scaling laws as its source.

* *Spectrum*

The frequency content of the spectrogram on Figure 5a is also remarkable: energy is present at relatively high frequencies of 7 to 12 Hz, 20 to 25 s into the signal. This is in contrast with the case of the 09:40 aftershock of comparable body-wave magnitude, whose spectrum is peaked at 5 Hz. Note in particular that these high-frequency components occur approximately mid-way into the signal; this would be predicted by the model of a block sliding on an inclined plane (HASEGAWA and KANAMORI, 1987), accelerating from a standstill and then slowing down to a stop, in which the highest particle velocities are reached at the center of the source time series. In contrast, wave packets from small-magnitude dislocations reflect very short rise times and generally feature a decay of frequency with time, illustrative of near-source scattering and accentuated in the case of *T* waves by their dispersion during propagation in the SOFAR channel. Finally, when combined with a total slip of $\approx$ 1 km (SWEET and SILVER, 2003), the total duration of the *T* wavetrain (47 s) would suggest average sliding velocities on the order of 25 m/s, which would in turn correspond to accelerations of $\approx 2 \mathrm{m/s^2}$, an acceptable figure on a slope estimated at 15° (SWEET and SILVER, 2003).

* *Amplitude*

On the other hand, the scale bars on Figure 5 show that the spectral amplitudes of the 09:02 *T* waves are only marginally larger than those of the 09:40 aftershock, and remain about 50 times smaller than those of the mainshock.

• Other records

In addition to the WK31 hydrophone records, we gathered as many records as possible from seismic stations located close to shore, either on Pacific Islands or along the rim of the ocean, in the configuration of the so-called *T*-phase stations (OKAL, 2001a). These are listed in Table 2, and spectrograms are presented on Figure 6. SOFAR propagation from the Bismarck Sea to some of the best receiving sites in the Pacific Basin (including Pomariorio, French Polynesia; Christmas Island;

Table 2

T-wave records at hydroacoustic and seismic stations

Location	Code	Nature of sensor	Network	Epicentral distance (km)	Estimated land path (km)	Record plotted on
Stations recording the 09:02 event						
Wake Hydrophone	WK31	Hydrophone	PIDC	3635		Fig. 5
Wake Island	WAKE	Broadband seismic	IRIS	3658	3	Fig. 6a
Guam	GUMO	Broadband seismic	IRIS	1863	43	Fig. 6b
Erimo, Japan	ERM	Broadband seismic	IRIS	4990	211	Fig. 6c
Petropavlovsk-Kamchatskiy, Russia	PET	Broadband seismic	IRIS	6407	280	Fig. 6d
Mount Rainier, Oregon	RAIO	Broadband seismic	IRIS	10645	164	Fig. 6e
Van Inlet	VIB	High-frequency seismic	PIDC	9973	41	Fig. 6f
Stations recording the mainshock (08:49) but not the 09:02 event						
Monterey OBS	MCGR	Ocean-bottom seismic	MBARI	10720	0	
Pin-lang, Taiwan	TWGB	Broadband seismic	Taiwan	3645	29	
Stations recording T waves after reflection						
Christmas Island	XMAS	Broadband seismic	IRIS	6762	8	
Haleakala, Maui	HLK	Broadband seismic	PeleNet	7225	27	

and most Hawaiian sites) is blocked at the source by the Admiralty Islands and adjoining structures (see Fig. 7), although reflected *T* phases are detectable at Christmas and Maui.

As shown on Figure 6, the frequency content of the 09:02 *T* phases recorded at the various stations shows a high degree of variability, reflecting the overland propagation following the acoustic-to-seismic conversion near the receiver. Table 2 documents that the land path traveled by the converted wave can vary substantially, reaching lengths of more than 150 km at RAIO, PET, and ERM (these estimates were obtained from a combined interpretation of arrival times of *T* phases and nearshore bathymetry). As discussed for example by TALANDIER and OKAL (1998) and OKAL (2001b), the nature of the converted wave and the characteristics of its on-land propagation are controlled by local structures on a scale comparable to the acoustic wavelengths involved (200 m at

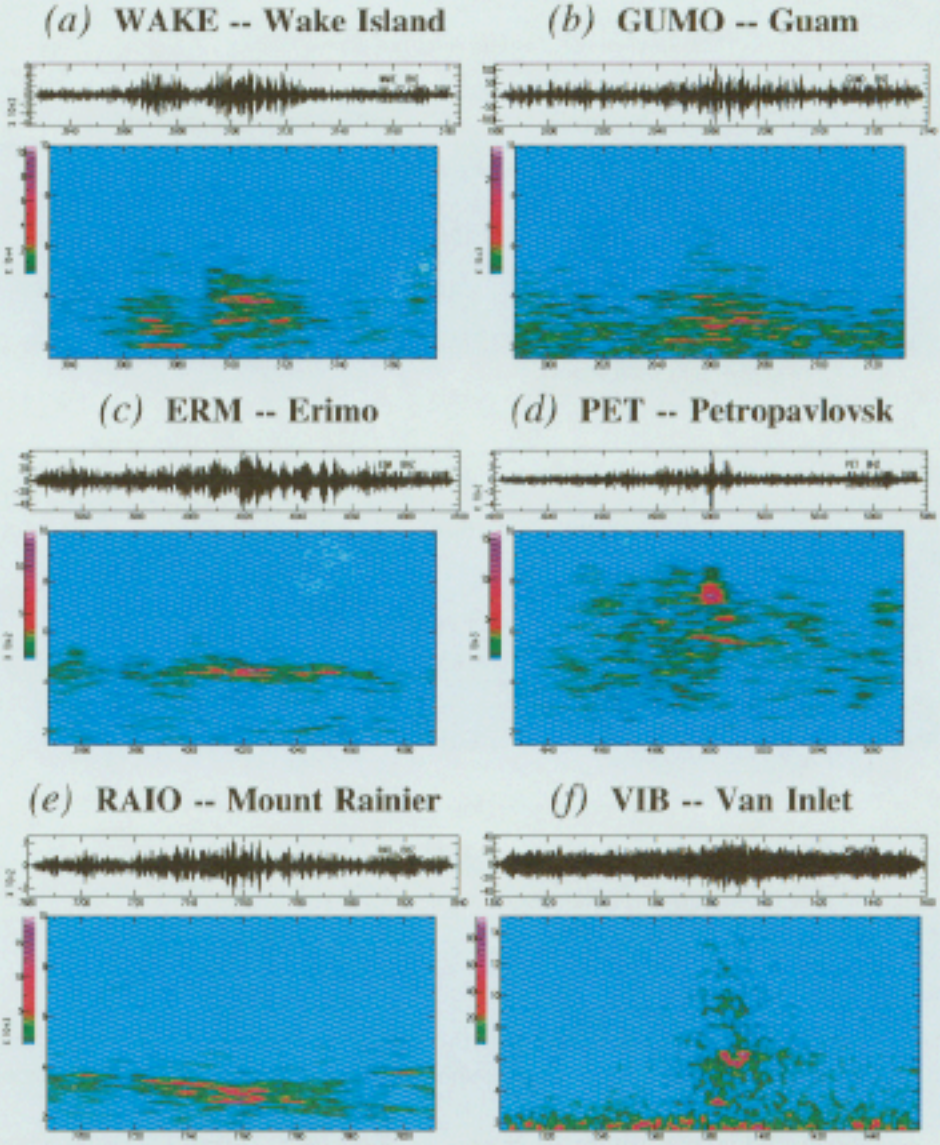

Figure 6

Spectrograms of *T* phases from the 09.02 event recorded at Pacific seismic stations. (a): WAKE (Wake Island); (b): GUMO (Guam); (c): ERM (Erimo, Hokkaido, Japan); (d): PET (Petropavlovsk-Kamchatskiy, Russia); (e): RAIO (Mount Rainier, Oregon); (f): VIB (Van Inlet, B.C., Canada). In all cases, the processed window lasts 160 seconds; the frequency band is 1.5–10 Hz, except at VIB (1.5–15 Hz) which records on a higher frequency channel.

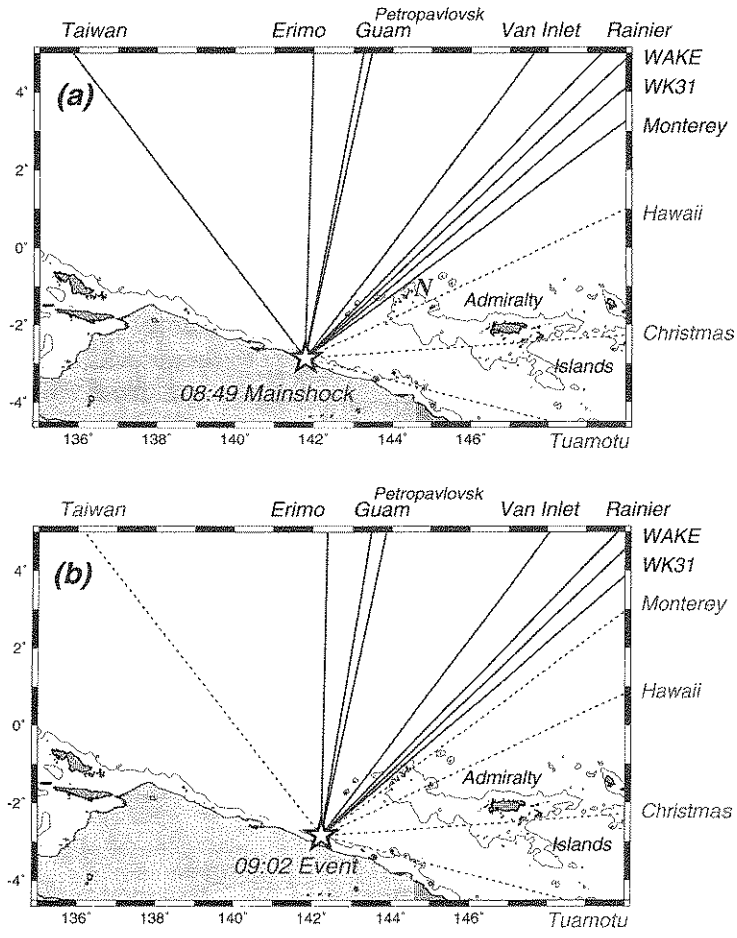

Figure 7

(a): Source-side blockage of T waves from the mainshock epicenter. The thin continuous line is the 1200-m isobath, representative of the axis of the SOFAR channel. Solid lines show great circle paths from the 08:49 NEIC epicenter to those stations where its T waves are recorded; the grey dashed lines show the paths to stations failing to record, or where the T wave involves a significant off-great circle reflection (Christmas; Maui). Note that the pattern is readily explained by source-side blockage at the Admiralty Islands. (b): Case of the 09:02 event. The absence at T waves at Monterey can be readily explained by blockage at the Ninigo Islands ("N" on frame (a)), but no structure can explain blockage along the path to TWGB (Taiwan).

7 Hz), and hence largely unknown. Figure 6 shows for example that the land paths can be regarded as a bandpass filter ($f \approx 4$ Hz) at ERM, as a low-pass filter at RAIO, but retain high frequencies of 7 to 10 Hz at both PET and VIB, these properties being uncorrelated with the length of the land path. Rather, it is probable that the retention of high frequencies in the T phase at PET, despite a land path reaching 280 km, expresses

favorable channeling through an efficient waveguide immediately below the Mohorovičić discontinuity.

The uncertainty surrounding the exact nature of the acoustic-to-station conversion and of the subsequent on-land propagation over distances reaching several hundred km, makes it impossible to invert *T*-phase arrival times in order to more precisely relocate the source of the 09:02 *T* phase. Rather, we simply verified that the observed arrival times were in all cases compatible with a legitimate conversion scenario. On the other hand, the duration of the various wavetrains analyzed on Figure 6 was found to be comparable to that measured on the WK31 record (Fig. 5), and thus to support the conclusion that the 09:02 source cannot be a simple dislocation of magnitude $m_b = 4.4$.

An additional intriguing observation is that we failed to detect 09:02 *T* phases at two Pacific sites which recorded powerful signals from the mainshock: Pin-lang, Taiwan (TWGB) and the Monterey Bay Ocean Bottom Seismometer (MCGR). The absence of signal at the latter is readily explained if we place the 09:02 source at the amphitheater, 42 km eastwards of the mainshock: this results in blockage by the Ninigo Islands (1.3°S; 144.4°E; "N" on Fig. 7a), which the *T* ray from the 08:49 epicenter just manages to avoid. This interpretation is confirmed by the weak amplitude of the 09:09 *T* waves at MCGR, which are expected to be generated mid-way between the 08:49 epicenter and the amphitheater, and whose ray should thus be grazing the islands.

On the other hand, selective blockage at Taiwan of *T* waves from the 09:02 event cannot be explained by an island or underwater ridge obstructing the path of the *T* wave (in particular, the main aftershock doublet at 09:09–09:10 generated *T* phases observed at TWGB). Rather, it must be attributed to the mechanism by which the acoustic energy is transferred to the water column in the epicentral area. A slump taking place inside the amphitheater would be expected to emit an acoustic signal directly inside the cavity into the water body of the ocean. Note in particular that the depth of the slump below sea level (1200 to 1800 m) is perfectly matched to that of the SOFAR channel, ensuring efficient excitation of acoustic energy into the wave guide. But this signal could leave the source only in the direction where the amphitheater is open to the high seas—to the north and northeast. To the northwest, in the azimuth of Taiwan, the western walls of the cavity, as mapped by SWEET and SILVER (2003), will essentially block propagation. This blockage would not be effective if the source was underground, since it could then illuminate seismically a larger section of the ocean floor, including presumably the seaside slope of the western wall of the cavity, and explaining the generation of a *T* phase in the azimuth of Taiwan by the main aftershock doublet.

4. Discussion

The principal characteristics of the *T*-wave signal recorded at the hydrophone station WK31—duration and frequency content—cannot be reconciled with the

reported body-wave magnitude of the event ($m_b = 4.4$). Rather, we have shown that the model of a slump taking place on the southern wall of the amphitheater mapped by TAPPIN *et al.* (1999) successfully explains these characteristics. Furthermore, these properties are generally supported by observations at other Pacific sites, instrumented with seismometers, in the geometry of a so-called *T*-phase station (OKAL, 2001a), and they are also generally comparable to the observations of the far-field hydroacoustic signatures of small underwater Hawaiian landslides reported by CAPLAN-AUERBACH *et al.* (2001).

We were also able to confirm several properties of the 09:02 event by studying its *P*-wave arrival at the seismic station WAKE, located on Wake atoll. From the epicentral area to the island receiver, the *P* wave travels as the oceanic P_n mode, identified as particularly efficient for regional-to-long distance propagation of high-frequency energy by WALKER (1977) (who called this phase "P_o") and TALANDIER and BOUCHON (1979). Figure 8 compares the spectrograms of the 09:02 and 09:40 *P* waves at the seismic station WAKE. The former features a duration of 40 s, which is in excellent agreement with the 47 s of the more dispersed acoustic *T* wave at the nearby hydrophone WK31; in contrast, the regular $m_b = 4.5$ aftershock has a P_o phase lasting no more than 13 s. We also confirm the occurrence of the highest frequency pulse (4.5 Hz for this record) about mid-way into the phase, in excellent agreement with the acoustic results.

We thus propose that the fresh slump identified inside the amphitheater by TAPPIN *et al.* (1999) and mapped by SWEET and SILVER (2003) actually took place at 09:02 GMT on 17 July 1998, thirteen minutes after the mainshock, and that this event was the source of the local catastrophic tsunami. As discussed by HEINRICH *et al.* (2000) and SYNOLAKIS *et al.* (2002), hydrodynamic models using the geometry and timing of the slump (with its estimated volume of 4 km^3) successfully predict the three characteristics of the observed run-up: its amplitude of 10 to 15 m along the coast, its rapid decay with distance along the coast, and the general timing of the arrival of the wave at the shore, neither of which can be explained by a dislocation occurring at the time of the mainshock.

How unique is the 09:02 event?

This interpretation of the 09:02 event as a slump responsible for the generation of the catastrophic tsunami requires a discussion of the uniqueness of its *T*-wave characteristics: in other words, we must establish that the event is indeed unique. For this purpose, we examined 15 hours of data at WK31, *i.e.*, the entire remainder of the GMT Julian day 1998:198, and in particular the *T* waves generated by the 40 aftershocks listed by the NEIC posterior to the main aftershock doublet at 09:09–09:10, the largest events having a reported magnitude $m_b = 4.7$ (at 18:17 and 18:50). Of those, six events (which may have had an on-land epicenter) did not generate *T* waves recordable at WK31, and one (at 11:28:51) corresponded to a gap in recording.

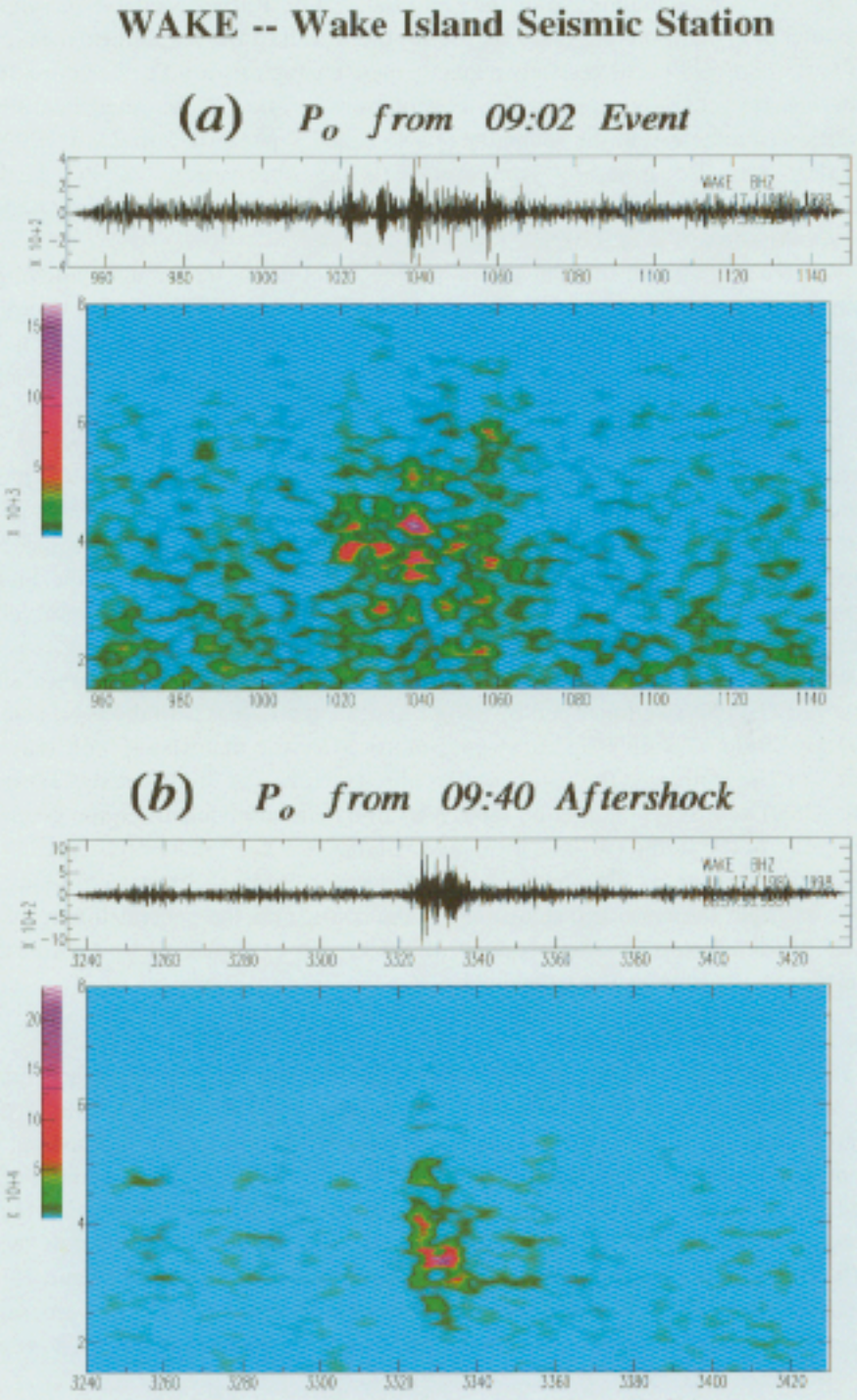
WAKE -- Wake Island Seismic Station
(a) P_o from 09:02 Event
WAKE BHZ
(b) P_o from 09:40 Aftershock
WAKE BHZ

Of the remaining 33 sources, we could find only four earthquakes with *T* waves at WK31 lasting between 37 and 47 s, while all remaining 29 shocks (including the 09:06 aftershock, whose timing could have made it a potential candidate for the source of the tsunami) have *T* waves of "regular duration," *i.e.*, comparable to those of the 09:40 aftershock featured on Figure 5c (13 s). The four events with longer *T* waves all have spectral amplitudes at least one order of magnitude lower than those of the 09:02 event. Their locations are shown as triangles on Figure 2. They are:

* *Event at 09:29:14; 2.82°S, 141.82°E*

This earthquake relocates at the western end of the mainshock rupture. It is part of a series of puffs of energy lasting more than 300 s, but is the only one whose *T* waves last more than 20 s.

* *Event at 10:51:50; 2.85°S, 142.06°E (m_b = 4.3)*

This shock relocates essentially at the 09:02 epicenter; it could involve a rockslide or small slump on the Western wall of the amphitheater.

* *Event at 12:15:10 (m_b = 3.2)*

This small event could not be meaningfully relocated, with its error ellipse extending more than 150 km in the NNW-SSE direction. *T* waves at WK31 last 47 s, but at a level 100 times lower than for the 09:02 slump.

* *Event at 13:52:55; 3.00°S, 142.26°E (m_b = 4.5)*

This earthquake relocates North of Malol, with its error ellipse intersecting the canyon surveyed by R.V. Kairei (TAPPIN *et al.*, 1999). Its *T* wave at WK31 lasts 47 s, but with a spectral amplitude 30 times less than its 09:02 counterpart. This event may be interpreted as having triggered a small landslide or slump along the walls of the canyon.

In summary, we find that the 09:02 slump is clearly unique (among aftershocks, and discounting the large 09:09–09:10 doublet) in amplitude rather than in nature: we document that several events with comparable *T*-wave signatures but much lower amplitudes, did take place in the general area off the Sandaun coast on that day. We interpret them as minor underwater rockslides or slumps; their occurrence would certainly be expected in the aftermath of a sizable mainshock. Only the 09:02 slump was of a size sufficient to generate a locally destructive tsunami.

In conclusion, the present study identifies the 09:02 event as featuring singular source characteristics which can be reconciled with the occurrence of a major slump on the southern wall of the amphitheater identified by TAPPIN *et al.* (1999). In this respect, our work allows the timing of the occurrence of the slump mapped by SWEET and SILVER (2003), and which the shipboard surveys could only describe as "fresh."

◀

Figure 8

Spectrogram of the regional oceanic phase P_o (WALKER, 1977) recorded at the Wake Island seismic station from the 09:02 event (a) and the 09:40 aftershock (b). In both instances, we use a 200-s window analyzed in the frequency band $1.5 < f < 8$ Hz. Note the longer duration, higher frequency spectrum and lower amplitude of the 09:02 signal.

By suggesting that slumps may have specific and enhanced T-wave signatures while at the same time generating locally catastrophic tsunamis, we give a new impulse to the longstanding idea that T-wave and tsunami excitation may somehow be correlated. This was first suggested by EWING *et al.* (1950), based on their intuition that the excitation of both types of waves would require an extremely shallow source. However, WADATI and INOUYE (1953) countered this suggestion based on the observation of T waves from on-land sources, and we now know that the complex mechanics of T-wave generation can result in substantial T waves even from the deepest earthquakes (OKAL and TALANDIER, 1997, 1998). Also, TALANDIER (1966) has shown in the case of the Kuriles event of 20 October 1963 that a "tsunami earthquake," characterized by enhanced tsunami generation (relative to its surface waves) was actually deficient in T-wave excitation, a conclusion confirmed in the case of recent tsunami earthquakes such as Nicaragua (1992) or Peru (1996) (OKAL *et al.*, 2001). In summary, in the case of elastic dislocations, little if any correlation can be expected between the excitation of T waves (by the highest-frequency components of the source spectrum), and tsunamis (by their static or lowest-frequency components). On the other hand, a slump such as the 09:02 event is of course a completely different source, which being in contact with the water column, possesses the potential for direct excitation of acoustic energy into the SOFAR channel.

The idea that major tsunamis could be generated by underwater slumps is far from new: it goes back to such early visionaries as MILNE (1898) and MONTESSUS DE BALLORE (1907), with GUTENBERG (1939) arguing that slumps were indeed the main generator of tsunamis. By contrast with subaerial events such as the Mount St. Helens landslide (KANAMORI *et al.*, 1984), underwater slumps are generally impossible to witness directly; thus only a handful of such events have been documented and thoroughly studied, mostly on the basis of the observation of cable breaks or turbidity currents. For example, HOUTZ (1962) modeled the 1953 tsunami at Suva, Fiji as generated by an underwater slump estimated at 0.3 km^3, and HASEGAWA and KANAMORI (1987) modeled the 1929 Grand Banks earthquake and tsunami as involving a 500 km^3 submarine landslide. Similarly, AMBRASEYS (1960) proposed that the tsunami of 09 July 1956 at Amorgos in the Southern Aegean Sea emanated from a landslide, a conclusion based on reports of turbidity in the seawater, and upheld by recent marine surveys (PERISSORATIS and PAPADOPOULOS, 1999). Finally, SOLOV'YEV *et al.* (1992) identified tsunami waves on tidal gauge records in Southern Spain, following the land-based 1954 and 1980 Algerian earthquakes, the former having triggered in the Mediterranean Sea a turbidity current documented by numerous cable breaks (HEEZEN and EWING, 1955).

Apart from those few well-documented cases, several authors have speculated that landslides or slumps may have played a role in the generation of other significant tsunamis. These would include the still unresolved case of the 1946 Aleutian event (KANAMORI, 1985; PLAFKER *et al.*, 2002), the 1975 Kalapana earthquake on the southern coast of Hawaii (EISSLER and KANAMORI, 1987), and a few other intriguing

events such as the 22 June 1932 aftershock of the large Colima–Jalisco earthquake of 03 June 1932.

It is probable that underwater landslides and slumps are ubiquitous phenomena on the ocean floor, and that the seismic and acoustic record of the past few decades includes literally myriads of them. As noted for example by AMBRASEYS (1960), the deformation field of a slump is dipolar in nature, and therefore, the tsunami that it raises affects mostly the near field. As such, only those slump events close enough to a populated shoreline may generate a detectable tsunami and thus be recognized. Yet, any assessment of the tsunami risk posed by underwater slumps requires accurate models of their population statistics, and possible recurrence patterns. Such investigations clearly represent a major challenge in the field of coastal hazards, which may constitute the scientific legacy of the catastrophic tragedy in Papua New Guinea.

Acknowledgments

I thank Costas Synolakis for arranging my participation in the Post-Tsunami Field Survey (under funding from the National Science Foundation), and for many subsequent discussions. I am grateful to an anonymous reviewer for constructive comments. *T*-wave records used in this study were obtained from the IRIS data management center, the POSEIDON data center, the Prototype International Data Center of the Comprehensive Nuclear Test Ban Treaty, or kindly provided by Cecily Wolfe (PELEnet), Jesse Williams (MBARI), and Bor-Shouh Huang (Taiwan network). Several figures were drawn using the GMT software (WESSEL and SMITH, 1991). Some aspects of this research were supported by the Defense Threat Reduction Agency, under contract DTRA01-00-C-0065.

REFERENCES

AMBRASEYS, N. N. (1968), *The Seismic Sea Wave of July 9, 1956 in the Greek Archipelago*, J. Geophys. Res. *65*, 1257–1265.

CAPLAN-AUERBACH, J., FOX, C. G., and DUENNEBIER, F. K. (2001), *Hydroacoustic Detection of Submarine Landslides on Kilauea Volcano*, Geophys. Res. Lett. *28*, 1811–1813.

DAVIES, H. L. (1998), *The Sissano Tsunami*, Univ. Papua New Guinea, Port Moresby.

DZIEWONSKI, A. M., EKSTRÖM, G., and MATERNOVSKAYA, N. (1999), *Centroid-moment Tensor Solutions for July–September*, 1998, Phys. Earth Planet. Inter. *114*, 99–107.

EISSLER, H. K. and KANAMORI, H. (1987), *A Single-force Model for the 1975 Kalapana, Hawaii Earthquake*, J. Geophys. Res. *92*, 4827–4836.

EWING, W. M., WOOLLARD, G. P., VINE, A. C., and WORZEL, J. L. (1946), *Recent Results in Submarine Geophysics*, Geol. Soc. Am. Bull. *57*, 909–934.

EWING, W. M., TOLSTOY, I., and PRESS, F. (1950), *Proposed Use of the T Phase in Tsunami Warning Systems*, Bull. Seismol. Soc. Am. *40*, 53–58.

GUTENBERG, B. (1939), *Tsunamis and Earthquakes*, Bull. Seismol. Soc. Am. *29*, 117–126.

HASEGAWA, H. S. and KANAMORI, H. (1929), *Source Mechanism of the Magnitude 7.2 Grand Banks Earthquake of November 18, 1929: Double-couple or Submarine Landslide*? Bull. Seismol. Soc. Am. *77*, 1984–2004.

HEEZEN, B. C. and EWING, M. (1955), *Orléansville Earthquake and Turbidity Currents*, Bull. Am. Assoc. Petrol. Geol. *39*, 2505–2514.

HEINRICH, P., PIATANESI, A., HÉBERT, H., and OKAL, E. A. (2000), *Near-field Modeling of the July 17, 1998 Event in Papua New Guinea*, Geophys. Res. Lett. *27*, 3037–3040.

HOFFMAN, I., SYNOLAKIS, C. E., and OKAL, E. A. (2002), *Systematics of the Distribution of Tsunami Run-up along Coastlines in the Near-field for Dislocation Sources with Variable Parameters*, Eos, Trans. Am. Geophys. Un. *83*, (22), WP54 (abstract).

HURUKAWA, N., TSUJI, Y., and WALUYO, B. (2003), *The 1998 Papua New Guinea Earthquake and its Fault Plane Estimated from Relocated Aftershocks*, Pure Appl. Geophys., *160*, 1829–1841.

HOUTZ, R. E. (1962), *The 1953 Suva Earthquake and Tsunami*, Bull. Seismol. Soc. Am. *52*, 1–12.

KANAMORI, H. (1985), *Non-double-couple Seismic Source*, Proc. XXIIIrd Gen. Assemb. Intl. Assoc. Seismol. Phys. Earth Inter. p. 425, Tokyo, (abstract).

KANAMORI, H., GIVEN, J. W., and LAY, T. (1984), *Analysis of Seismic Waves Excited by the Mount St. Helens Eruption of May 18, 1980*, J. Geophys. Res. *89*, 1856–1866.

KIKUCHI, M., YAMANAKA, Y., ABE, K., MORITA, Y., and WATADA, S. (1998), *Source rupture process of the Papua New Guinea earthquake of July 17, 1998 inferred from teleseismic body waves*, Eos. Trans. Amer. Geophys. Un. *79 (45)*, F573 (abstract).

MCCUE, K. F. (1998), *An AGSO Perspective on PNG's Tsunamigenic Earthquake of 17 July 1998*, Austral. Geol. Intl. *9*, 1–2.

MILNE, J., *Earthquakes and other Earth movements*, 376 pp. (Paul, Trench, Trübner and Co., London, 1898).

MONTESSUS DE BALLORE, F. La Science Séismologique (A. Colin, Paris, 1907), 579 pp.

OKAL, E. A. (2001a), *T-phase Stations for the International Monitoring System of the Comprehensive Nuclear-Test Ban Treaty: A Global Perspective*, Seismol. Res. Lett. *72*, 186–196.

OKAL, E. A. (2001b), *Converted T Phases Recorded on Hawaii from Polynesian Nuclear Tests: A Preliminary Report*, Pure Appl. Geophys. *158*, 457–474.

OKAL, E. A. and TALANDIER, J. (1989), M_m: *A Variable Period Mantle Magnitude*, J. Geophys. Res. *94*, 4169–4193.

OKAL, E. A. and TALANDIER, J. (1997), *T Waves from the Great 1994 Bolivian Deep Earthquake in Relation to Channeling of S-Wave Energy up the Slab*, J. Geophys. Res. *102*, 27,421–27,437.

OKAL, E. A. and TALANDIER, V. (1998), Correction to "*T Waves from the Great 1994 Bolivian Deep Earthquake in Relation to Channeling of S-wave Energy up the Slab*," J. Geophys. Res. *103*, 2793–2794.

OKAL, E. A., ALASSET, P.-J., HYVERNAUD, O., and SCHINDELÉ, F. (2003), *The Deficient T Waves of Tsunami Earthquakes*, Geophys. J. Intl. *152*, 416–432.

PERISSORATIS, C. and PAPADOPOULOS, G. (1999), *Sediment Instability and Slumping in the Southern Aegean Sea and the Case History of the 1956 Tsunami*, Mar. Geol. *161*, 287–305.

PLAFKER, G., OKAL, E. A., and SYNOLAKIS, C. E. (2002), *A New Survey of the 1946 Aleutian Tsunami in the Near-Field: Evidence for a Large Underwater Landslide at Davidson Bank*, Seismol. Res. Lett. *73*, 259 (abstract).

SOLOV'YEV, S. L., CAMPOS-ROMERO, M. L., and PLINK, N. L. (1992), *Orléansville Tsunami of 1954 and El Asnam Tsunami of 1980 in Alboran Sea (Southwestern Mediterranean Sea)*, Izv. Earth Phys. *28*, 739–760.

SWEET, S. and SILVER, E. A. (2003), *Tectonics and Slumping in the Source Region of the 1998 Papua New Guinea Tsunami from Seismic Reflection Images*. Pure Appl. Geophys. this issue.

SYNOLAKIS, C. E., BARDET, J.-P., BORRERO, J. C., DAVIES, H. L., OKAL, E. A., SILVER, E. A., SWEET, S., and TAPPIN, D. (2002), *The Slump Origin of the 1998 Papua New Guinea Tsunami*, Proc. Roy. Soc. London, Ser. A, *458*, 763–789.

TALANDIER, J. (1966), *Contribution à la prévision des Tsunamis*, C. R. Acad. Sci. Paris, *263B*, 940–942.

TALANDIER, J. and BOUCHON, M. (1979), *Propagation of High-frequency P_n Waves at Great Distances in the Central and South Pacific, and its Implication for the Structure of the Lower Lithosphere*, J. Geophys. Res. *84*, 5613–5620.

TALANDIER, J. and OKAL, E. A. (1998), *On the Mechanism of Conversion of Seismic Waves to and from T Waves in the Vicinity of Island Shores*, Bull. Seismol. Soc. Am. *88*, 621–632.

TALANDIER, J. and OKAL, E. A. (2001), *Identification Criteria for Sources of T Waves Recorded in French Polynesia*, Pure Appl. Geophys. *158*, 567–603.

TAPPIN, D. R. and 18 co-authors (1999), *Sediment Slump Likely Caused 1998 Papua New Guinea Tsunami*, Eos, Trans. Am. Geophys Un. *80*, pp. 329, 334 and 340.

WADATI, K. and INOUYE, W. (1953), *On the T Phase of Seismic Waves Observed in Japan*, Proc. Japan Acad. *29*, 47–54.

WALKER, D. A. (1977), *High-frequency P_n and S_n Phases Recorded in the Western Pacific*, J. Geophys. Res. *82*, 3350–3360.

WESSEL, P. and SMITH, W. H. F. (1991), *Free Software Helps Map and Display Data*, Eos, Trans. Am. Geophys. Un. *72*, pp. 441 and 445–446.

WYSESSION, M. E., OKAL, E. A., and MILLER, K. L. (1991), *Intraplate Seismicity of the Pacific Basin*, 1913–1988, Pure Appl. Geophys. *135*, 261–359.